

DTIC FILE COPY

2

PORT DOCUMENTATION PAGE

Form Approved  
OMB No 0704-0188

**AD-A222 628**

|   |  |   |                         |
|---|--|---|-------------------------|
| 2b. DECLASSIFICATION/DOWNGRADING SCHEDULE   |  | 1e. RESTRICTIVE MARKINGS  |                         |
| 4. PERFORMING ORGANIZATION REPORT NUMBER(S)<br>No. 3  |  | 3. DISTRIBUTION/AVAILABILITY OF REPORT<br>Approved for public release and sale; its distribution is unlimited |                         |
| 5. MONITORING ORGANIZATION REPORT NUMBER(S)   |  | 7a. NAME OF MONITORING ORGANIZATION<br>Office of Naval Research   |                         |
| 6a. NAME OF PERFORMING ORGANIZATION<br>Univ. of North Carolina  | 6b. OFFICE SYMBOL<br>(if applicable)     | 7b. ADDRESS (City, State, and ZIP Code)<br>Chemistry Division, Code 1113<br>Arlington, VA 22217               |                         |
| 6c. ADDRESS (City, State, and ZIP Code)<br>Chemistry Dept., CB #3290, Venable Hall<br>Univ. of North Carolina<br>Chapel Hill, NC 27599-3290                                       |  | 9. PROCUREMENT INSTRUMENT IDENTIFICATION NUMBER<br>N00014-89-J-1169, 4131036                                  |                         |
| 8a. NAME OF FUNDING/SPONSORING ORGANIZATION<br>ONR  | 8b. OFFICE SYMBOL<br>(if applicable)     | 10. SOURCE OF FUNDING NUMBERS   |                         |
| 8c. ADDRESS (City, State, and ZIP Code)<br>Chemistry Division, Code 1113<br>Arlington, VA 22217   |  | PROGRAM ELEMENT NO.   | PROJECT NO.             |
| 11. TITLE (Include Security Classification)<br>Structure and Dynamics of Water at the Pt(111) interface:<br>Molecular Dynamics Study  |  | TASK NO.  | WORK UNIT ACCESSION NO. |
| 12. PERSONAL AUTHOR(S)<br>K. Raghavan, K. Foster, K. Motakabbir and M. Berkowitz  |  |   |                         |
| 13a. TYPE OF REPORT<br>Interim Technical  | 13b. TIME COVERED<br>FROM _____ TO _____ | 14. DATE OF REPORT (Year, Month, Day)   | 15. PAGE COUNT          |
| 16. SUPPLEMENTARY NOTATION<br>Submitted to J. Chem. Phys.   |  |   |                         |
| 17. COSATI CODES  |  | 18. SUBJECT TERMS (Continue on reverse if necessary and identify by block number)                             |                         |
| FIELD   | GROUP                                    | Molecular Dynamics, Computer Simulation,<br>Water-Metal Interface, (JK) ←                                     |                         |
|   |  |   |                         |
| 19. ABSTRACT (Continue on reverse if necessary and identify by block number)<br><br>SEE ATTACHED ABSTRACT   |  |   |                         |
| 20. DISTRIBUTION/AVAILABILITY OF ABSTRACT<br><input checked="" type="checkbox"/> UNCLASSIFIED/UNLIMITED <input type="checkbox"/> SAME AS RPT. <input type="checkbox"/> DTIC USERS |  | 21. ABSTRACT SECURITY CLASSIFICATION<br>Unclassified/unlimited  |                         |
| 22a. NAME OF RESPONSIBLE INDIVIDUAL<br>Dr. M. Berkowitz   |  | 22b. TELEPHONE (Include Area Code)<br>(919)-962-1218  | 22c. OFFICE SYMBOL      |

DTIC  
ELECTE  
JUN 1 1990  
S B D  
Cb

OFFICE OF NAVAL RESEARCH

Grant N00014-89-J-1169

R&T Code 4131036

Technical Report #3

"Structure and Dynamics of Water at the Pt(111) interface:  
Molecular Dynamics Study"

by

K. Raghavan, K. Foster, K. Motakabbir and M. Berkowitz

Submitted to

J. Chem. Phys.

Department of Chemistry  
University of North Carolina  
Chapel Hill, NC 27599

May 18, 1990

Reproduction in whole or in part is permitted for  
any purpose of the United States Government.

This document has been approved for public release  
and sale; its distribution is unlimited

## ABSTRACT

An analytical form of the interaction potential between rigid water-rigid metal surface, which takes into account the surface symmetry and its corrugation is developed. Using this potential the structure and dynamics of water at Pt (111) interface is investigated. At 300K the adjacent to the metal surface water layer displays solid-like properties. Patches of ice-like structure embedded in this layer are observed in the simulation. The next two layers of water display ordering similar to ice-I. Beyond these three layers the structure and dynamics of water is bulk like. → 1473

April 1990  
J. Chem. Phys.  
(submitted)

**STRUCTURE AND DYNAMICS OF WATER AT THE Pt(111) INTERFACE:  
MOLECULAR DYNAMICS STUDY.**

K. Raghavan, K. Foster, K. Motakabbir and M. Berkowitz

Department of Chemistry, University of North Carolina, Chapel Hill, NC 27599, USA

## Abstract

An analytical form of the interaction potential between rigid water-rigid metal surface, which takes into account the surface symmetry and its corrugation is developed. Using this potential the structure and dynamics of water at Pt (111) interface is investigated. At 300K the adjacent to the metal surface water layer displays solid-like properties. Patches of ice-like structure embedded in this layer are observed in the simulation. The next two layers of water display ordering similar to ice-I. Beyond these three layers the structure and dynamics of water is bulk like.

|                      |                                     |
|----------------------|-------------------------------------|
| <b>Accession For</b> |                                     |
| NTIS GRA&I           | <input checked="" type="checkbox"/> |
| DTIC TAB             | <input type="checkbox"/>            |
| Unannounced          | <input type="checkbox"/>            |
| Justification _____  |                                     |
| By _____             |                                     |
| Distribution/        |                                     |
| Availability Codes   |                                     |
| Dist                 | Avail and/or<br>Special             |
| A-1                  |                                     |



## 1. Introduction

A detailed molecular level description of structure and dynamics of water next to metallic surfaces is of fundamental importance for electrochemistry, catalysis, and corrosion studies. Structural details about water monolayer-metal surface interface can be obtained using different experimental techniques, described in a review by Thiel and Madey [1]. In the case of bulk water-metal interface, where no molecular level information is available from experiment, computer simulations can play a very significant role. In these simulations the form of water-metal interaction potential is crucial in determining the structure and dynamics of water at the interface. Very often to represent this interaction an image charge method is used in the simulations [2-4]. This results in an orientation of one of the water hydrogens towards the surface [3], in contradiction to experimental observations which show that water tends to situate with its oxygen atom located next to the metallic surface and its hydrogens pointing away [1]. Theoretical calculations on bonding of water to transition metal clusters support the same conclusion [5,6]. Based on one of such calculations of water on Pt cluster [6], Spohr and Heinzinger developed an interaction potential for water-platinum atom [7]. Using this potential, Spohr performed a molecular dynamics simulation of a slab of water between two Pt (100) surfaces [8]. In Spohr's simulation the Pt surfaces were explicitly represented by 550 Pt atoms. Recently we have developed a water-platinum surface potential [9], which takes into account the symmetry of Pt surface and its corrugation. This potential allowed us to concentrate on the motion of water molecules, replacing all Pt atoms by an effective external field. Comparison of structural data from our simulation with Spohr's simulation of water at Pt (100) interface displayed a very good agreement between two simulations, despite that Spohr used a flexible water model and we used a rigid water model.

While Spohr's work and our initial work simulate water-Pt (100) interface, most

experimental data are available for water-Pt (111) interface [1]. This interface is also more interesting, since the nearest-neighbor Pt-Pt distance is commensurate with the water-water distance and Pt(111) surface is hexagonal; all these facts favor creation of ice structure at the interface. Such ice-like structure was observed in high-vacuum studies of water layers on Pt surface at temperatures around 150K [1]. The main motivation for our present study was to see how much of this ice structure remains at the interface of bulk water and Pt (111) surface at room temperature.

## 2. Potential Energy Surface

The multi-dimensional potential energy surface is represented by water-water and water-surface interaction potentials. The water-water potential we use in our simulation is determined by SPC/E model, which represents quite nicely bulk properties of water [10,11]. To obtain the interaction of water molecule with Pt (111) surface, we have used individual atoms in water-surface potentials. The O-Pt (111) surface and H-Pt (111) surface potentials are given by:

$$V_{O,Pt} = f_0(z) + f_1(z)Q_1(x,y) + f_2(z)Q_2(x,y) \quad (1a)$$

$$V_{H,Pt} = g_0(z) + g_1(z)Q_1(x,y) + g_2(z)Q_2(x,y) \quad (1b)$$

where

$$Q_1(x,y) = \cos 2\pi s_1 + \cos 2\pi s_2 + \cos 2\pi s_3 \quad (2a)$$

$$Q_2(x,y) = \sin 2\pi s_1 + \sin 2\pi s_2 - \sin 2\pi s_3 \quad (2b)$$

and

$$s_1 = \sqrt{2}/a [ x - y/\sqrt{3} ] \quad (3a)$$

$$s_2 = 2\sqrt{2}y / (\sqrt{3} \cdot a) \quad (3b)$$

$$s_3 = s_2 + s_1 \quad (3c)$$

In equations (3)  $a=0.392$  nm which is the Pt lattice constant.

The functional forms of  $f$  and  $g$  are given by:

$$\begin{aligned}
 f_0(z) &= A_1 \exp[ -\beta_1(z - z_m) ] + A_2 \exp[ -\beta_2(z - z_m) ] \\
 f_1(z) &= A_3 \exp[ -\beta_3(z - z_m) ] + A_4 \exp[ -\beta_4(z - z_m) ] \\
 f_2(z) &= A_5 \exp[ -\beta_5(z - z_m) ] + A_6 \exp[ -\beta_6(z - z_m) ] \\
 g_0(z) &= A_7 \exp[ -\beta_7(z - z_m) ] \\
 g_1(z) &= A_8 \exp[ -\beta_8(z - z_m) ] \\
 g_2(z) &= A_9 \exp[ -\beta_9(z - z_m) ] \tag{4}
 \end{aligned}$$

In the above equations (4) the values of the parameters were obtained by a fit to the Spohr-Heinzinger potential [7] and are given in table 1. In equations (3) and (4)  $x, y, z$  are coordinates of the atom in the water molecule.

On a Pt (111) surface one can distinguish four binding positions for the water molecule (see figure 1). The preferential adsorption site is on the top of platinum atom (site A) with an adsorption energy of -40.7 kJ/mol. The energies of adsorption on hollow sites B and C are -27.1 kJ/mol and -23.9 kJ/mol respectively, while the adsorption energy on bridge site D is -26.1 kJ/mol. These energies are in qualitative agreement with the recently calculated energies of adsorption of  $H_2O$  on Ni(111) [12]. To provide a general picture of the water - Pt (111) interaction its potential is displayed in figures 2 and 3. Figure 2 displays the variation of the water - Pt(111) potential in  $z$ -direction (direction perpendicular to the plane of Pt surface), while the contour plot of the shape of the interaction potential in the  $x, y$  plane can be seen in figure 3a. Figure 3b shows the contour plot obtained by using Spohr-Heinzinger potential which involves explicit summation of contributions from every  $H_2O$  - Pt atom interaction. Interaction of one water molecule with 2688 atoms of Pt arranged in fcc (111) structure was included in the sum.

Comparison of figures 3a and 3b shows that our fit reproduces rather well the symmetry and shape of H<sub>2</sub>O - Pt(111) surface interaction.

### 3. Molecular Dynamics Simulation

To study structural and dynamical properties of the water-Pt interface molecular dynamics simulation of SPC/E water bounded by two Pt (111) surfaces was performed. Since the interatomic distance between Pt atoms (~0.277 nm) is commensurate to the distance between water molecules in ice and the hexagonal structure of the lattice is capable of promoting ice structure we had to find a unit cell which will not obstruct a possible creation of ice-like structures at the interface. Therefore, we have chosen a hexagonal prism as our molecular dynamics box with the hexagon as its base. The hexagonal base serves as a unit cell for a two dimensional ice-like structure of water on Pt (111) surface and it is shown in figure 4. This structure, which allows the maximum coverage of the surface, was proposed by Doering and Madey [13]. As one can see from figure 4, the idealized structure of water on the Pt (111) surface is actually a bilayer with the first layer of the bilayer having all molecules in a "flip-up" position (position, in which water molecules have their dipoles pointing away from the surface), while the second layer, hydrogen bonded to the first layer is made up of "flip-up" and "flop-down" (dipole moments pointing towards the surface) waters.

The dimensions of the molecular dynamics box are as follows: The length of the hexagon side in the base is 2.24nm. In order to satisfy the form of water-Pt interaction potential given by equations (1)-(4) with parameter values from table 1 we had to place the first layer of Pt atoms at distances  $|z| = 1.5$  nm from the center, therefore we may say that the distance between Pt surfaces is 3 nm. The total number of water molecules in the simulation was adjusted until the density in the middle of the box was equal to the bulk density (1 g/cm<sup>3</sup>). That resulted in a total number of 1298 water molecules in our

simulation. The simulation was run for 20 ps of equilibration time followed by 40 ps of production run. The time step used was 2.5 fs. The molecular dynamics Verlet algorithm [14] with the Shake routine [15] was used to propagate the trajectories. A minimum image convention was used to calculate the interactions. Periodic boundary conditions, modified to account for the hexagonal shape of the unit cell were used in x and y directions. Since the size of the cell was rather large the long-range forces contribution was not included in the simulation. The temperature of the simulation was 300 K.

#### 4. Results

##### 4a. Structure

The oxygen and hydrogen density profiles obtained from the simulation are displayed in figure 5. The plot demonstrates that the results obtained from the right and the left part of the simulation box are symmetric as it should be expected. The oxygen density profile clearly shows two well separated peaks next to Pt surface. The first peak corresponds to an adsorbed water layer and the second peak is due to a layer that is hydrogen bonded to it. Although not as prominent as the two peaks next to the surface, a third peak corresponding to the third layer can also be distinguished. The first water layer, L1, located at  $1.10\text{nm} < |z| < 1.35\text{nm}$  has an average density of 1.47 g/cc and the average number of water molecules in this layer is 158, which is close to 150 water molecules in the ideal structure (see figure 4). The second layer, L2, occupies the region  $0.84\text{nm} < |z| < 1.10\text{nm}$ , its average density is 1.09 g/cc. The third layer, L3, occupies the region  $0.46 < |z| < 0.84\text{nm}$  and has the bulk density.

The density profiles from figure 5 and orientational distributions from figure 6 are instrumental in reconstruction of water structure in the lamina. To find more details on this structure the layer L1 was divided into two sublayers and orientational distribution of

angles between water dipole vector and the normal vector pointing into Pt surface along z-direction was calculated. Also a distribution of angles between OH vector and surface normal vector was calculated. These two distributions are reproduced in figure 6 together with the distribution for other sublayers. For the first sublayer of the first layer ( $1.25\text{nm} < |z| < 1.35\text{nm}$ ) most of the molecules have their dipole moments pointing slightly away from the surface and OH vectors are mostly parallel to the surface with a slight tilt. That means that most of the molecules of the first sublayer are "flip-up" type molecules. The distribution of dipole moments for the second sublayer ( $1.15\text{nm} < |z| < 1.25\text{nm}$ ) is bimodal which clearly indicates that the sublayer has "flip-up" and "flop-down" molecules. "Flop-down" molecules are hydrogen bonded to "flip-up" molecules of the first sublayer and the hydrogen atoms of "flip-up" molecules of the second sublayer of the first layer are hydrogen bonded to the second layer. These are the hydrogens which are giving a small peak in hydrogen density profile curve in the region  $1.12\text{nm} < |z| < 1.18\text{nm}$ . The second small hydrogen peak in the region  $1.02\text{nm} < |z| < 1.12\text{nm}$  is due to the hydrogens of the second layer. The positions of the peaks for the dipole orientation curves indicate that the planes of water molecules in the first layer are close to being parallel to the surface. Therefore if the hexagonal ice-like structure of water next to the surface exists, it should be mostly flat, with a very slight puckering.

To study the structure of the wider second layer we have divided it into three sublayers. The first sublayer of the second layer ( $1.05\text{nm} \leq |z| \leq 1.15\text{nm}$ ) includes all these water molecules which serve as a bridge between layers L1 and L2 and there are not many of them. Most of the water molecules are found in the second and third sublayers of the second layer. The OH vector distribution and dipole distribution of the second sublayer of the second layer display an enhanced probability for the water molecule to point one of the OH vectors directly into the wall. Simultaneously, the second OH vector is pointing away from the wall in the direction that makes a tetrahedral angle towards the

first OH bond. The orientational distributions of the second and third sublayers of L2 are mirror images of one another with respect to  $\cos \theta = 0$ . Such behavior is expected if water would have an ice-I structure with the c-axis along the z-direction. Although the orientational distributions for these two sublayers in our simulations are broad, the maxima correspond to what would be expected for distributions in ice-I structure. In addition, we have also noticed that the distance between the second and third layers in our simulation is 0.35nm, which is the distance between layers in ice-I structure, and that the third layer has orientational distributions reminiscent of the second layer. Based on the preceding discussion we propose that water in the second and third layers display an ordering similar to that of ice-I. Similar ordering was observed by Lee *et al* [16] in their simulation of water next to hydrophobic wall.

To summarize, the following structure of water next to Pt(111) surface is proposed. At the surface around 80% of available adsorption sites are occupied by water. This value is consistent with the number from the ideal structure proposed by Doering and Madey [13]. In the ideal structure one observes regularly distributed patches of ice which are densely packed together. We have also observed some patching of hexagonal ice-like structures in our simulation (see below). Moving in z-direction into bulk the orientational and lateral ordering of water is not completely homogeneous and is biased towards the ordering observed in ice-I structure with its c-axis directed along z-direction. We believe that water has bulk-like structure beyond the third layer, although the dipole orientation plot shows slight anisotropy even in the middle of the lamina. This is similar to the nonuniformity of orientational properties observed by Valteau and Gardner [17]. We think that this preference is related to the use of minimum image boundary conditions in the simulations, although the possibility that the box length is not large enough should not be excluded.

One of the interesting questions related to the structure of hexagons of water on

the surface is the following: Given a hexagon what is its predominant conformation while adsorbed on the Pt(111) surface? For the hexagon ring one can distinguish between so-called "boat" and "chair" configurations. The following is an explanation of a means by which the hexagonal rings can be separated into families of "boat-like" and "chair-like" configurations.

The six dihedral angles of the hexagonal ring were focused on as variables determining the ring's conformation. Boats are readily distinguished from chairs by comparing their respective dihedral angle patterns. In the typical chair, the dihedral angle alternate between positive and negative values of values of equal magnitude as one goes around the ring, e.g.  $(-30^\circ, +30^\circ, -30^\circ, +30^\circ, -30^\circ, +30^\circ)$ . In the perfect boat conformation, a cyclical pattern of three angle values exists consisting of one positive and one negative value of equal magnitude and a third angle of  $0^\circ$ , i.e.  $(30^\circ, -30^\circ, 0^\circ, 30^\circ, -30^\circ, 0^\circ)$  or  $(0^\circ, -30^\circ, 30^\circ, 0^\circ, -30^\circ, 30^\circ)$  and all cyclic permutations. A "flat" or "coplanar" ring is neither a boat nor a chair; all of a "flat" ring's dihedral angle values are identically zero.

An arbitrary hexagonal ring of in thermal motion is seldom configured to match the descriptions of a perfect "chair", "boat", or "flat" ring. Consequently, ad hoc rules had to be drawn up to enable the characterization of rings into three categories. The rules employed were: (1) a hexagon having at least three dihedral angle values with absolute values less than  $10^\circ$  was considered "flat", (2) a hexagon having 3 positive and 3 negative dihedral angle values alternately interspersed and with no dihedral angle absolute values less than  $10^\circ$  was considered a "chair", (3) a hexagon with 2 dihedral angle values less than  $-10^\circ$ , 2 dihedral angle values greater than  $+10^\circ$  and 2 with absolute values less than  $10^\circ$ , cyclically disposed was considered a "boat", (4) a hexagon not fitting any of the 3 descriptions above was considered "flat".

We have performed a conformation analysis on the three hexagon rings, which are members of an ice-like patch on the surface. The analysis was done using 40

conformations, each separated by 0.25 ps, and the results are presented in Table 3. Since the cut-off angle discussed above (10° angle) is arbitrary, we present the results for two values of this angle: 10° and 20°. While the quantitative results do depend on the value of the angle, the qualitative result is independent of it. Most of the hexagons are "flat", as we have anticipated it (see section 4a). This is due to the strong water-Pt interaction, which flattens the hexagon ring. When the ring is not flat it prefers a "boat" conformation.

#### 4b. Dynamics

Perhaps the most illustrative exposition of the structure and dynamics of water in our simulation is the scatter plots in figures 7a-7d. In these figures a dot has been drawn every 0.25 ps at the (x,y) position of the each oxygen atom. Figure 7a depicts positions of waters in xy plane for L1 layer, 7b for L2 layer, 7c for L3 layer and 7d for the 0.35nm layer in the middle of the box. The molecules in the layer L1 are repeating the structure of underlying fcc Pt(111) surface and their motions are mostly oscillations about equilibrium positions. While for the second layer some ordering is still observed and the configuration space coverage is not homogeneous, the density distribution looks more like in L3. To have some quantitative estimates related to the diffusional motion of water molecules, we have calculated apparent diffusion coefficients for molecules in L1, L2, L3 and in the middle of the box. The mean square displacements in x and in z-directions for each of these four layers are represented in figure 8, and the effective diffusion coefficients obtained from the formulas

$$D_{xy} = \lim_{t \rightarrow \infty} \frac{\langle \Delta x^2 \rangle + \langle \Delta y^2 \rangle}{4t}$$

$$D_z = \lim_{t \rightarrow \infty} \frac{\langle \Delta z^2 \rangle}{2t}$$

are given in Table 2.

In our calculations of mean square displacement in the layer, we considered the molecule as belonging to the layer even when the molecule crossed the boundaries of the layer, but remained outside no longer than 1 ps. No substantial diffusion is observed in the layer next to the wall, while a large anisotropy in diffusion coefficient is observed for the second layer. As one can see the water molecules in L2 are more mobile in the direction parallel to the metal surface, than in the perpendicular direction. The anisotropy in diffusion is greatly reduced for the third layer and is nearly disappeared for molecules in the bulk-like part of the box. Some degree of anisotropy still remains, in the bulk-like part of the box which may be due to the way we calculate the effective diffusion coefficient, but it may also reflect the real dynamic anisotropy in the middle of the lamina.

A close look at the structure of water in figure 7a reveals the presence of hexagonal ice-like structures. Figure 9, which is just an enlarged figure 7a, clearly displays patches of the hexagonal rings. These patches are similar to the ones present in the ideal structure from figure 4. To get a better feeling on the stability of ice-like patches next to the Pt surface we have looked at few snapshots of the water structure in L1. We observed that the location of the ice-like patches was not changed but the number of hexagonal rings in the patch was changing with time.

Since there are empty adsorption sites on the Pt surface, there is a possibility for the motion of the water molecule from one adsorption site to the neighboring site. Indeed, we have observed such motion. To understand how such motion occurred we have followed a few trajectories of the particles that move from one adsorption site to another. In all cases we have considered, the molecules move away from the surface to the edge of layer L1, often recrossing into layer L2, where the rather fast ( $\sim 1$  ps) exchange of adsorption site occurs. A typical trajectory illustrating water molecule hopping between two adsorption sites is shown in figure 10. In spite of this hopping motion between the neighboring sites, a patch of ice-like structure next to the surface which was stable during the whole 40 ps

of the simulation time was observed.

#### 4c. Hydrogen Bonding

To get further insight into the structure and dynamics of water between Pt walls we have performed a layer-wise hydrogen bond analysis on the water coordinates generated by the simulation. We have considered three water layers: L1, L2 and LB - layer next to the center ( $0.0\text{nm} < |z| < 0.3\text{nm}$ ). The analysis was performed on 80 configurations from a 40ps run. Two consecutive configurations were separated in time by 0.5ps.

For each layer we have computed inter-molecular energies for molecules that belong to the particular layer concerned and are within 0.323nm away. If the pair interaction energy was below  $V_{\text{H.B}} = -2.5$  kcal/mole, we considered the pair to be hydrogen bonded. In Table 4 we show the distribution of hydrogen bonds in different layers. It should be noted here that we have considered only those bonds for which both the molecules are in a single layer. That is why for layers L2 and L3 the peak is shifted to two hydrogen bonds per molecule, since other hydrogen bonds are made with the waters belonging to the neighboring layers. For the layer L1 the peak is on three hydrogen bonds per molecule, which is in agreement with what one would get from the calculation performed on the idealized structure.

Using a recently developed scheme [18], we have enumerated non-short circuited hydrogen bonded polygons (rings) for each layer. The distribution of these polygons is shown in Table 5. We can clearly see the distinctly flat nature of the distribution in L1 as opposed to the distribution in L2 and LB, where the peak is on pentagonal species. Keeping in mind that we have considered only those polygons which are defined entirely within a single layer, we can understand the abundance of pentagons in L2 and LB since they are the most planar rings. Near the wall, in L1 layer, due to the surface influence

we find also four and six membered hydrogen bonded rings.

Although hydrogen bonded polygons are only transient structural species we thought it would be interesting to investigate if any of these species may be found stable enough to be detectable, especially near the wall. For this purpose we calculated polygon survival times by explicitly identifying unique rings in subsequent configurations. In Table 6 we present the distribution of rings that survived for at least 0.5 ps. It also shows the maximum survival time defined by the longest time of survival of at least one member. As we can see in the layer near the wall at least one hexagon survived up to 12.5 ps where as in layers L2 and L3 none survived more than 1.5 ps. It should also be pointed out that in the layer near the wall although hexagon survived for longest duration, the survival times for pentagons (7.5 ps), quadrangles (6.5 ps) or even triangles (4.5 ps) are also significant.

### Summary and Conclusions

We have investigated the structure and dynamics of water confined between Pt(111) surfaces using molecular dynamics computer simulations method, with particular emphasis on the behavior of water at the water/metal interface. We have derived an analytical form of the interaction potential for the H<sub>2</sub>O/Pt(111) system which incorporates the corrugation of the Pt(111) surface. A hexagonal prism has been used as the simulation box instead of the cubic/rectangular box which is traditionally employed in molecular dynamics simulations. This was necessary in order to avoid the destruction of hydrogen bonding network along the x,y directions.

The oxygen and hydrogen density profiles along the direction perpendicular to the metal surface and orientational distributions for dipoles and OH vectors show that there are three ordered layers of water on the Pt(111) surface. The first layer which is adsorbed

on the surface exhibits patterns in which water forms ice-like structures consisting of hexagons with the oxygens bound to Pt atoms on the surface. The second layer of water which is hydrogen bonded to the first layer of adsorbed water molecules also shows the static ordering influenced by the template effect of the Pt(111) surface through the adsorbed layer. Although not as prominent as the the first two layers, there persists some ordering in the third layer of water that is hydrogen bonded to the second layer. Beyond this layer, transition to bulk behavior is noticed. The distributions of dipole and OH vectors, in conjunction with the density profiles suggest that the displayed ordering is similar to the one observed in ice-I.

The analysis we carried out on the hydrogen bond network using an energetic criterion also supports the static ordering of the adsorbed layer. It was found that, in the adsorbed layer six membered rings survive for a longer time than the fewer-membered rings, evidencing the influence of the template effect of the Pt(111) surface on the preferential creation of six membered rings among the water molecules. The ring structures formed in the second layer and beyond do not survive as long as the ones in the adsorbate layer.

Perhaps the most interesting result from the present study is a quick change in the behavior of water at the interface, which occurs over a distance of only few angstrom. While water displays solid-like behavior in a layer adsorbed on the surface the next to it water layer already displays liquid-like behavior. And this is indeed remarkable.

#### Acknowledgement

This work was supported by a grant from the Naval Research Office. The simulations were performed on a Cray YMP at the North Carolina Supercomputing Center. One of us (MLB) is grateful to Dr. L. Pratt for stimulating discussions.

## Literature:

- [1] P.A Thiel and T. E. Madey, Surf. Sci. Rept. 7, 211 (1987)
- [2] N.G. Parsonage and D. Nicholson, J. Chem. Soc. Faraday Trans. 2, 82, 1521 (1986); *ibid.* 83, 663 (1987)
- [3] A.A. Gardner and J.P. Valleau, J. Chem. Phys. 86, 4175 (1987)
- [4] J. Hautman, J.W. Halley and Y.-J. Rhee, J. Chem. Phys. 91, 467 (1989)
- [5] M.W. Ribarsky, W.D. Luedtke and U. Landman, Phys. Rev. B 32, 1430 (1985)
- [6] S. Holloway and K.H. Bennemann, Surface Sci. 101, 327 (1980)
- [7] E. Spohr and K. Heinzinger, Ber. Bunsenges. Physik. Chem. 92, 1358 (1988)
- [8] a). E. Spohr, J. Phys. Chem. 93, 6171 (1989)  
b). E. Spohr, Chem. Phys. 141, 87 (1990)
- [9] K. Foster, K. Raghavan and M. Berkowitz, Chem. Phys. Lett. 162, 32 (1989)
- [10] H.J.C. Berendsen, J.R. Grigera, and T.P. Straatsma, J. Phys. Chem. 91, 6269 (1987)
- [11] M. Rami Reddy and M. Berkowitz, Chem. Phys. Lett. 155, 173 (1989)
- [12] H. Yang and J.L. Whitten, Surf. Sci. 223, 131 (1989)
- [13] D.L. Doering and T.E. Madey, Surf. Sci. 123, 305 (1982)
- [14] L. Verlet, Phys. Rev. 98, 159 (1967)
- [15] J.P. Ryckaert, G. Ciccotti, and H.J.C. Berendsen, J. Comput. Phys. 23, 327 (1977)
- [16] C.Y. Lee, J.A. McCammon, and P. Rossky, J. Chem. Phys. 80, 4448,(1984)
- [17] J.P. Valleau and A.A. Gardner, J. Chem. Phys. 86, 4162 (1987)
- [18] K. Motakabbir and M. Berkowitz, J. Phys. Chem. Submitted

## Figure Captions:

1. A portion of fcc Pt(111) surface illustrating different binding sites. Solid circle represents the a-top site (site-A); Cross-hatched circle represents the three-fold hollow site (site-B) under which there is a Pt atom in the second layer; The circle with a plus sign represents the three-fold hollow site (site-C) under which there is no Pt atom in the second layer; The mid point of the solid line connecting two a-top sites represents the bridge site (site-D).

2. Interaction potential for water-Pt(111) surface shown for different binding sites as a function of distance along the normal to the Pt surface. (a) a-top site; (b) hollow site-B; (c) hollow site-C; (d) bridge site.

3. (a) Potential energy contours for the water-Pt(111) interaction. ( x-axis : -0.59 to 0.59 nm ; y-axis : -0.4 to 0.4 nm ). The contours are obtained using equations (1)-(4) with parameters given in Table 1. The values of the potential at points represented by a, b, and c are -40 kJ/mol, -27.1 kJ/mol and -23.9 kJ/mol respectively.

(b) Same as Fig. 3 (a) only obtained from the potential given in ref. [7].

4. Ideal structure of water bilayer on the surface of fcc Pt(111). The cross-hatched oxygens belong to the first layer of the bilayer and are "flip-up". The water molecules that have "+" sign belong to the second layer and are "flop-down". The rest of the water molecules in the second layer are "flip-up" with one of the hydrogens pointing in z-direction away from the Pt surface.

5. Oxygen (solid line) and hydrogen (dotted line) density profiles obtained from our simulation.

6. Distributions of dipole (solid line) and OH (dotted line) orientations as a function of  $\cos \theta$  ( $\theta$  is the angle between the dipole or OH vector and the inward normal to the metal surface).

(a)  $1.25 < z < 1.35$  nm; (b)  $1.15 < z < 1.25$  nm; (c)  $1.05 < z < 1.15$  nm; (d)  $0.95 < z < 1.05$  nm;  
 (e)  $0.85 < z < 0.95$  nm; (f)  $0.72 < z < 0.85$  nm; (g)  $0.59 < z < 0.72$  nm; (h)  $0.46 < z < 0.59$  nm;  
 (i)  $0.0 < z < 0.14$  nm;

7. Projection of positions of oxygen atoms on the xy plane (plane parallel to the Pt surface) for four different layers of water at different distances from the metal surface.

(a) adsorbate layer ( $1.10 < z < 1.35$  nm); (b) second layer ( $0.84 \text{ nm} < z < 1.10$  nm); (c) third layer ( $0.46 \text{ nm} < z < 0.84$  nm); (d) fourth layer ( $0.0 \text{ nm} < z < 0.35$  nm). The particle trajectories are 10 ps long.

8. Mean square displacement in x and z directions as a function of time for different bins in the simulation box.

|  |   |
|--|---|
| $\square$ $-\langle x^2(t) \rangle$ in a bin where $ z  < 0.46$ nm;        | $\circ$ $-\langle z^2(t) \rangle$ for $ z  < 0.46$ nm;                          |
| $\triangle$ $-\langle x^2(t) \rangle$ for $0.46 \text{ nm} < z < 0.84$ nm; | $\nabla$ $-\langle z^2(t) \rangle$ for $0.46 \text{ nm} < z < 0.84$ nm;         |
| $\diamond$ $-\langle x^2(t) \rangle$ for $0.84 \text{ nm} < z < 1.10$ nm;  | $\blacksquare$ $-\langle z^2(t) \rangle$ for $0.84 \text{ nm} < z < 1.10$ nm;   |
| $\bullet$ $-\langle x^2(t) \rangle$ for $1.10 \text{ nm} < z < 1.35$ nm;   | $\blacktriangle$ $-\langle z^2(t) \rangle$ for $1.10 \text{ nm} < z < 1.35$ nm. |

9. Same as figure 7a. The hexagonal ice-like patches are shown explicitly.

10. A typical trajectory showing the changes in x,y, and z coordinates for a water molecule hopping between two adsorption sites. Only oxygen atom coordinates are displayed.

Table 1

The parameters for H<sub>2</sub>O-Pt(111) potential

---

| kJ/mol                       | nm <sup>-1</sup>   |
|------------------------------|--------------------|
| $A_1 = 16.094$               | $\beta_1 = 33.541$ |
| $A_2 = -54.988$              | $\beta_2 = 9.653$  |
| $A_3 = -18.013$              | $\beta_3 = 32.205$ |
| $A_4 = 15.417$               | $\beta_4 = 30.557$ |
| $A_5 = -0.626$               | $\beta_5 = 7.127$  |
| $A_6 = -0.113$               | $\beta_6 = 14.357$ |
| $A_7 = 10.610$               | $\beta_7 = 9.630$  |
| $A_8 = 4.048 \times 10^{-2}$ | $\beta_8 = 24.192$ |
| $A_9 = 4.800 \times 10^{-4}$ | $\beta_9 = 26.295$ |

$$z_m = -1.233 \text{ nm}$$

Table 2

Effective diffusion coefficients for different bins (in units of  $10^{-5}$  cm<sup>2</sup>/sec).

---

|       | L1   | L2   | L3   | LB   |
|-------|------|------|------|------|
| $D_v$ | <0.1 | 1.58 | 2.20 | 2.46 |
| $D_i$ | <0.1 | 0.14 | 1.06 | 1.95 |

Table 3

Conformational analysis of hexagons in the ice-like patches.

---

| Cut-off angle (deg) | hexagon # | # of "boats" | # of "chairs" | # of "flats" |
|---------------------|-----------|--------------|---------------|--------------|
| 10                  | 1         | 3            | 2             | 35           |
|                     | 2         | 4            | 0             | 36           |
|                     | 3         | 0            | 1             | 39           |
| 20                  | 1         | 0            | 1             | 39           |
|                     | 2         | 4            | 0             | 36           |
|                     | 3         | 0            | 1             | 39           |

Table 4

Distribution of hydrogen bonds per molecule.

---

| n | Probability in: |        |        |
|---|-----------------|--------|--------|
|   | L1              | L2     | LB     |
| 0 | 0.0022          | 0.0372 | 0.0638 |
| 1 | 0.0450          | 0.2432 | 0.3068 |
| 2 | 0.3248          | 0.4654 | 0.4309 |
| 3 | 0.4926          | 0.2395 | 0.1709 |
| 4 | 0.1307          | 0.0111 | 0.0080 |
| 5 | 0.0031          | 0.0000 | 0.0000 |

Table 5

Distribution of hydrogen bonded polygons.

---

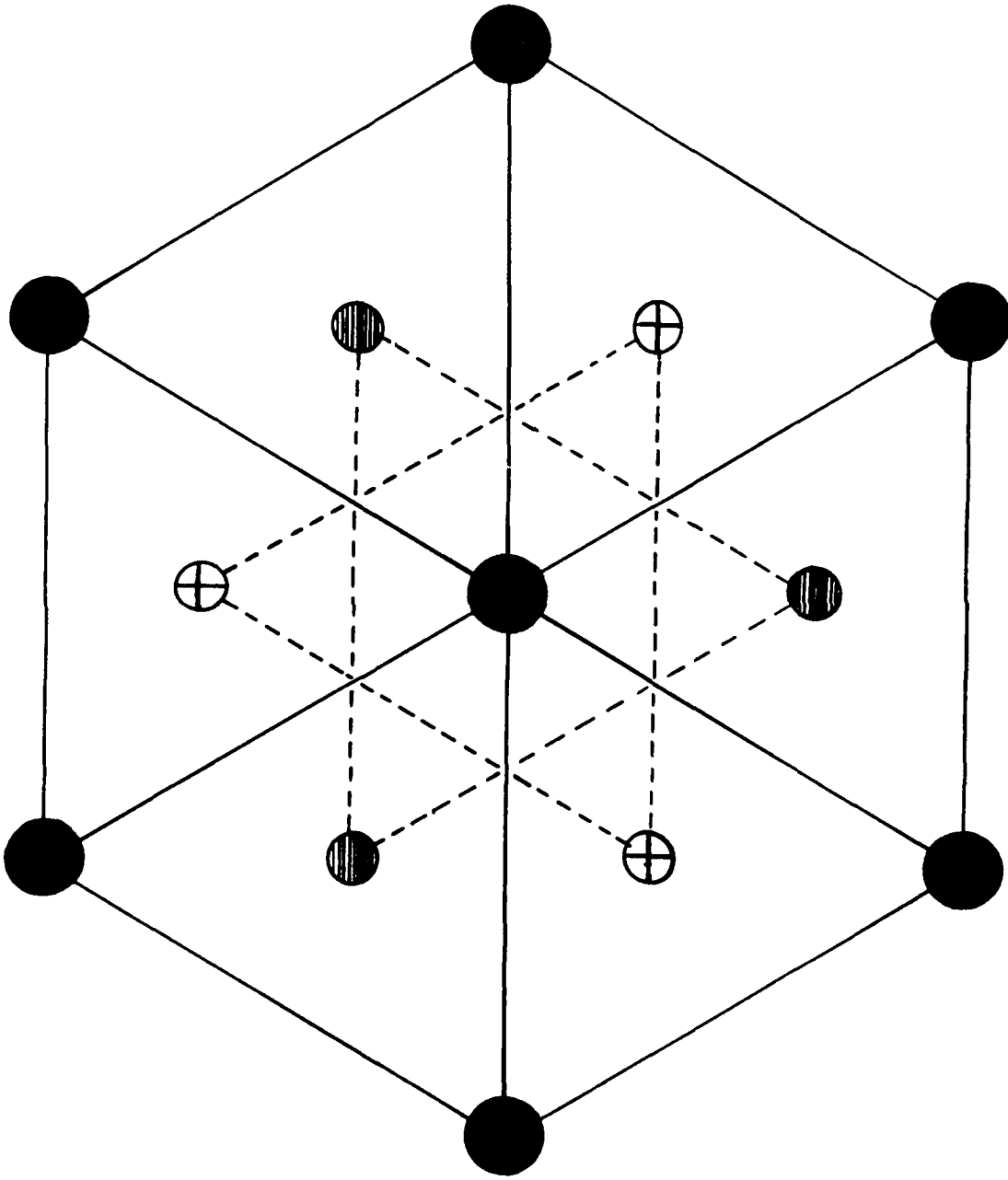
| Size | Probability in: |        |        |
|------|-----------------|--------|--------|
|      | L1              | L2     | LB     |
| 3    | 0.0799          | 0.0465 | 0.0941 |
| 4    | 0.1963          | 0.2095 | 0.2289 |
| 5    | 0.2056          | 0.3132 | 0.2510 |
| 6    | 0.2015          | 0.1646 | 0.1803 |
| 7    | 0.0852          | 0.0810 | 0.0982 |
| 8    | 0.0835          | 0.0707 | 0.0278 |
| 9    | 0.0597          | 0.0434 | 0.0378 |
| 10   | 0.0518          | 0.0378 | 0.0153 |
| 11   | 0.0366          | 0.0335 | 0.0041 |

Table 6

Distribution of rings that survived at least 0.5 ps and maximum survival times.

---

| Size | # of rings that survived<br>at least 0.5 ps |    |    | Maximum survival times in ps |     |     |
|------|---|----|----|------------------------------|-----|-----|
|      | L1  | L2 | LB | L1                           | L2  | LB  |
| 3    | 93  | 1  | 0  | 4.5                          | 0.5 | 0.0 |
| 4    | 256   | 20 | 6  | 6.5                          | 1.5 | 0.5 |
| 5    | 296   | 42 | 18 | 7.5                          | 1.5 | 1.5 |
| 6    | 263   | 13 | 11 | 12.5                         | 1.5 | 1.5 |
| 7    | 64  | 4  | 1  | 2.5                          | 1.5 | 1.5 |
| 8    | 51  | 2  | 1  | 3.5                          | 0.5 | 0.5 |
| 9    | 25  | 0  | 0  | 1.5                          | 0.0 | 0.0 |



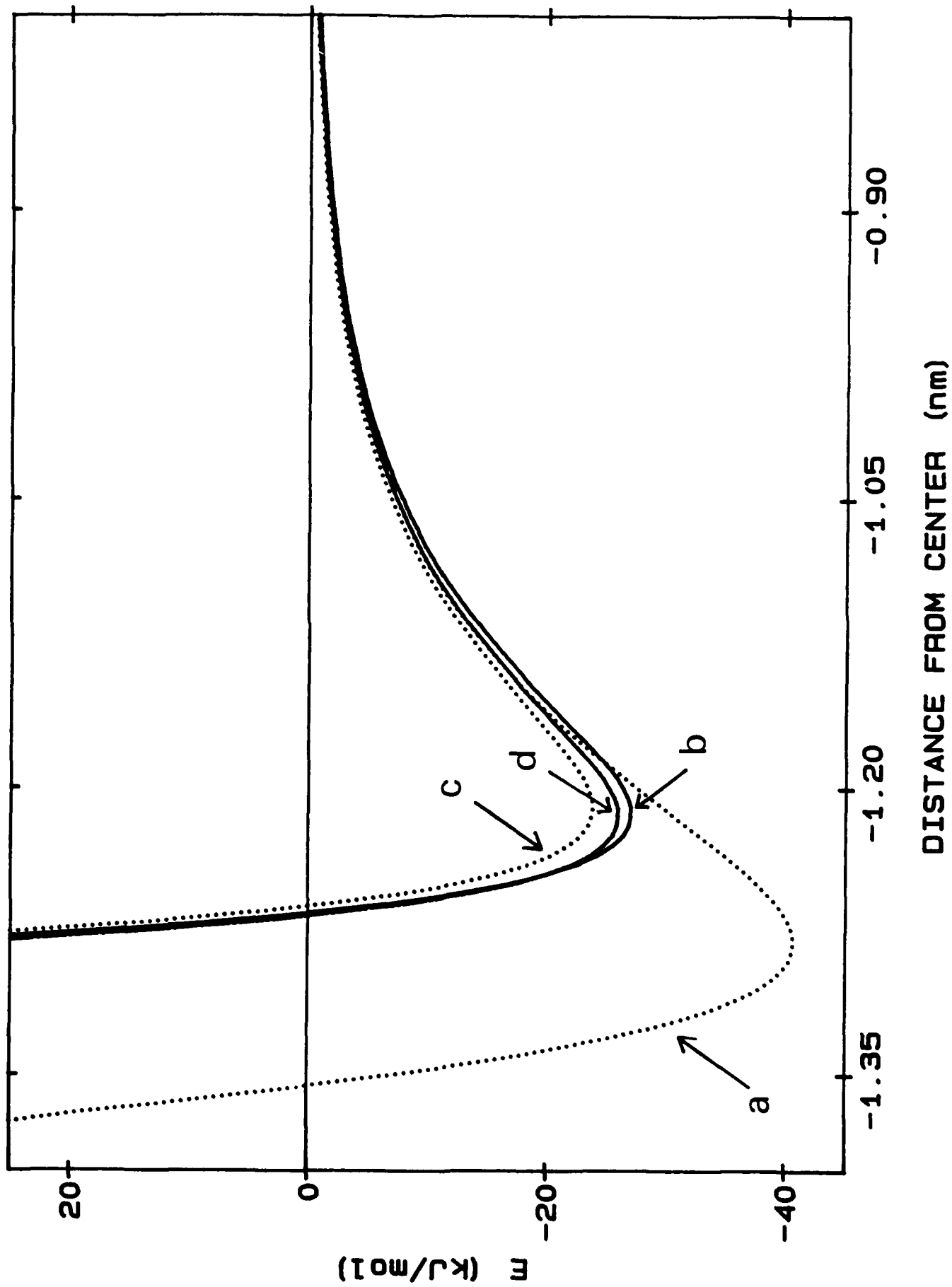
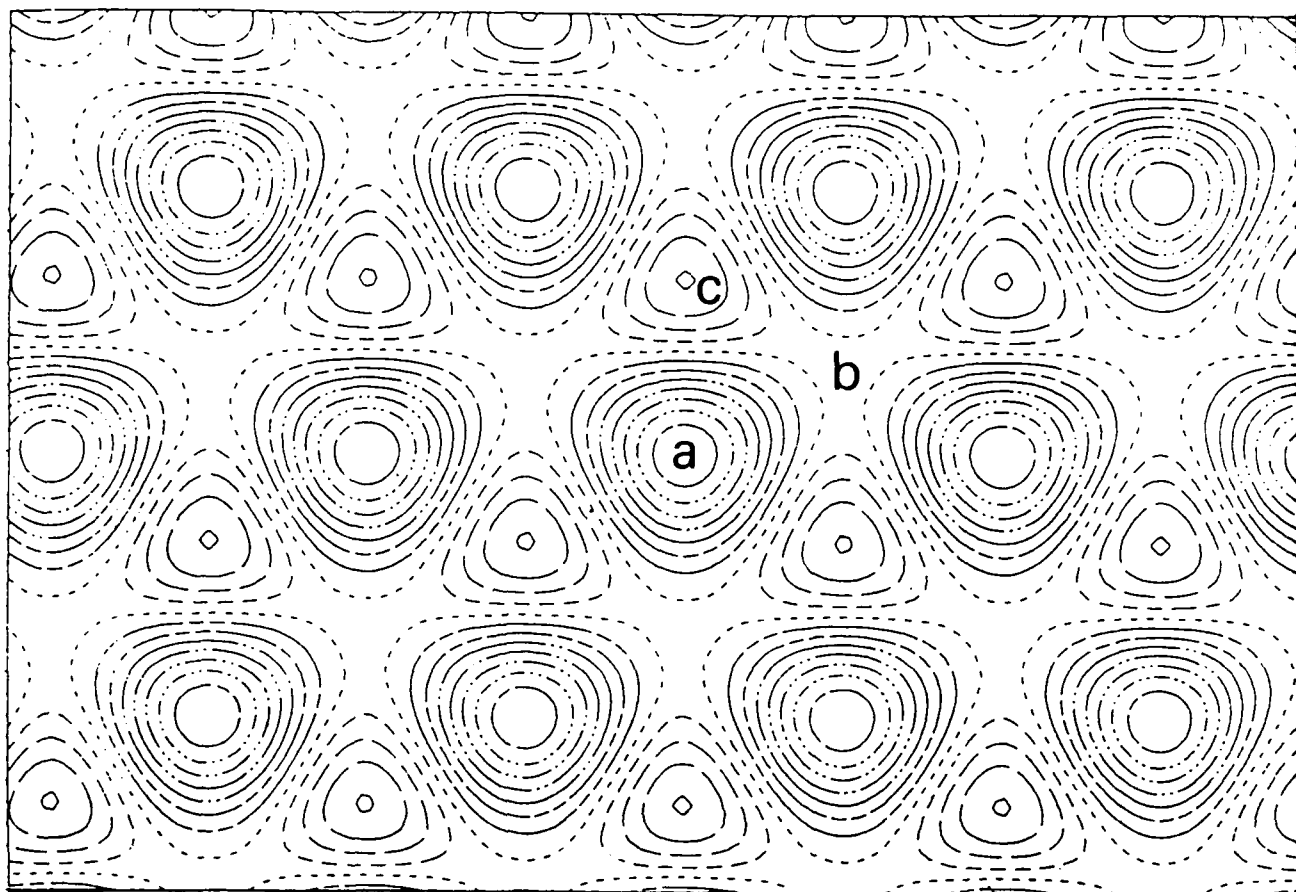
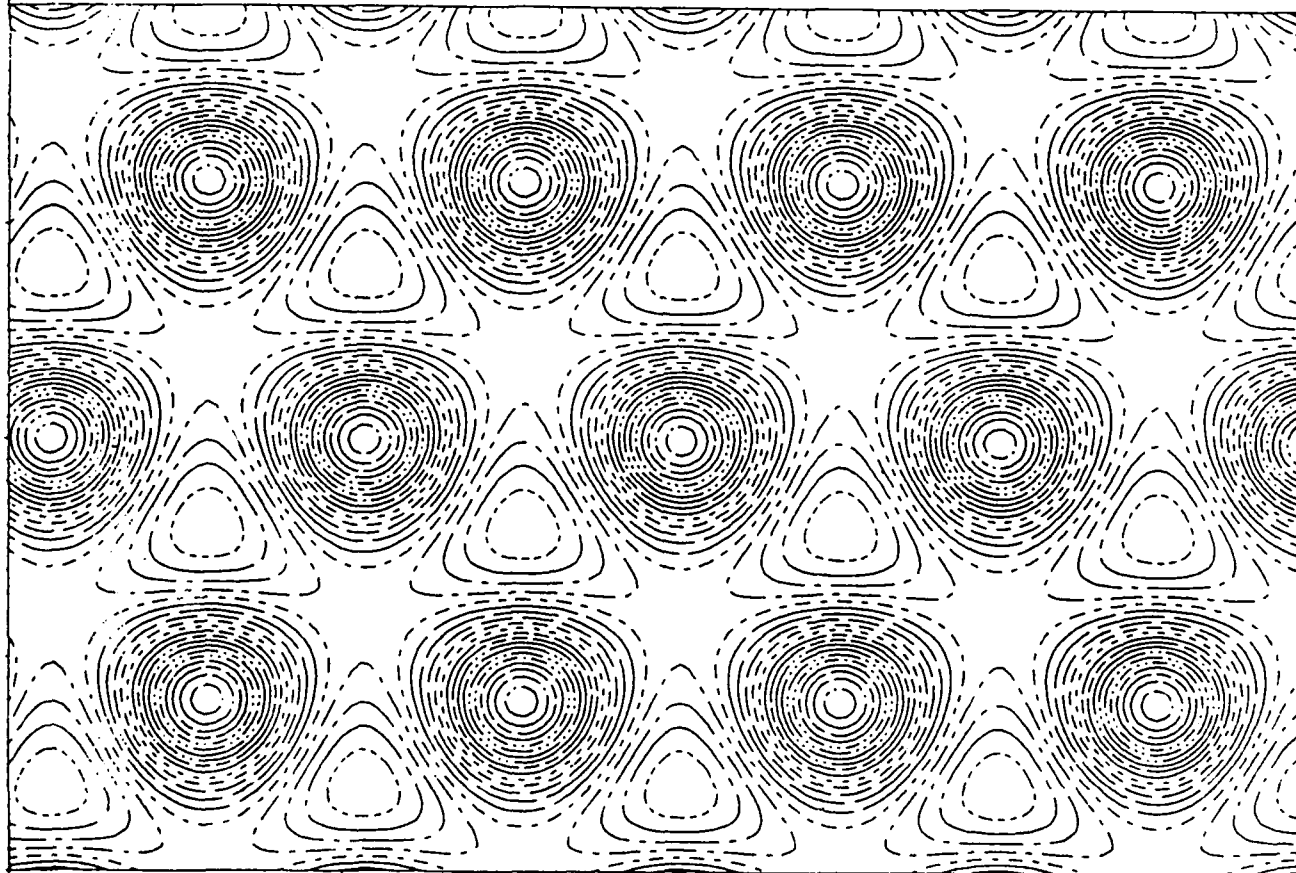


fig 2.

(a)



(b)



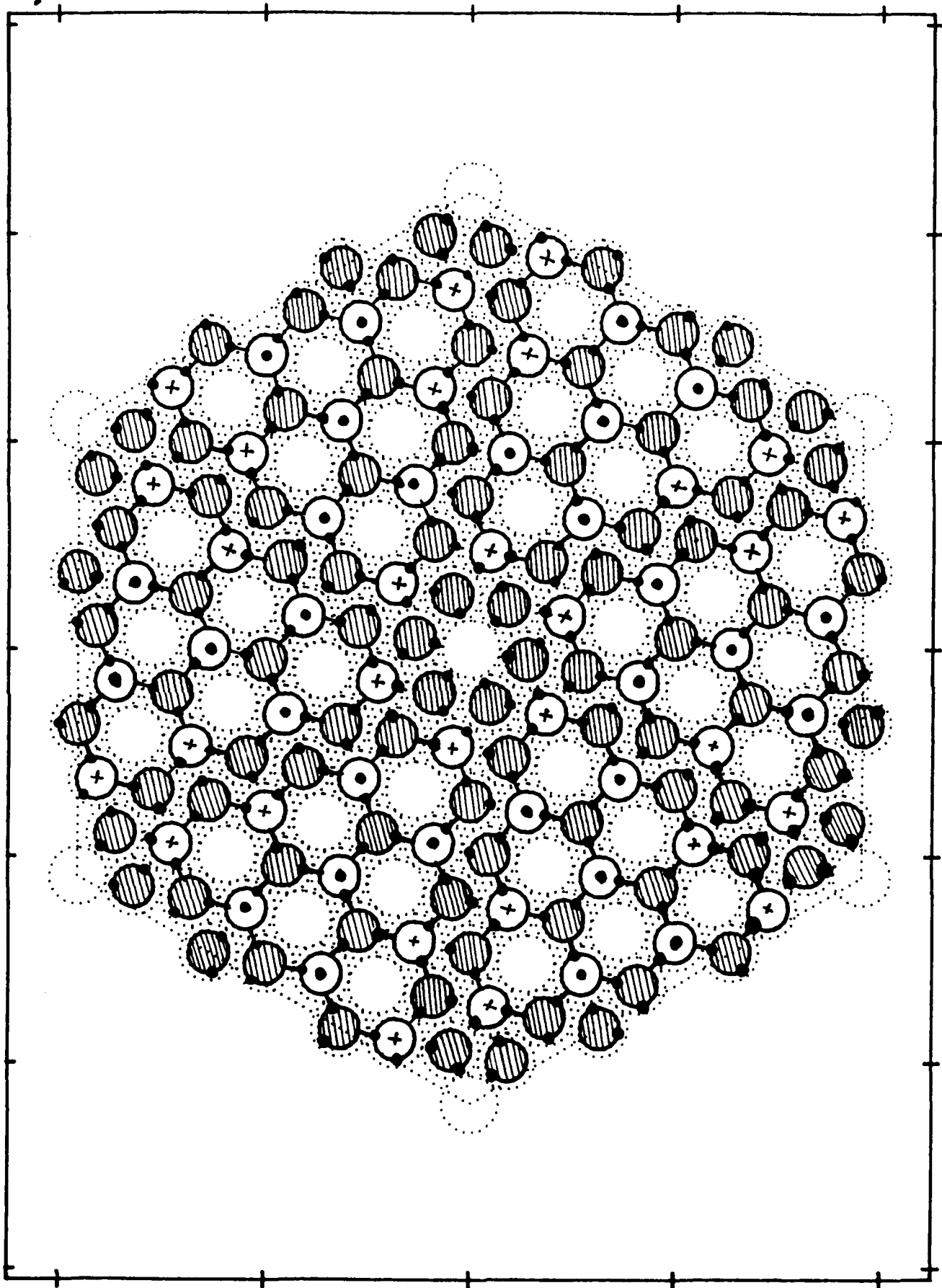


fig. 4

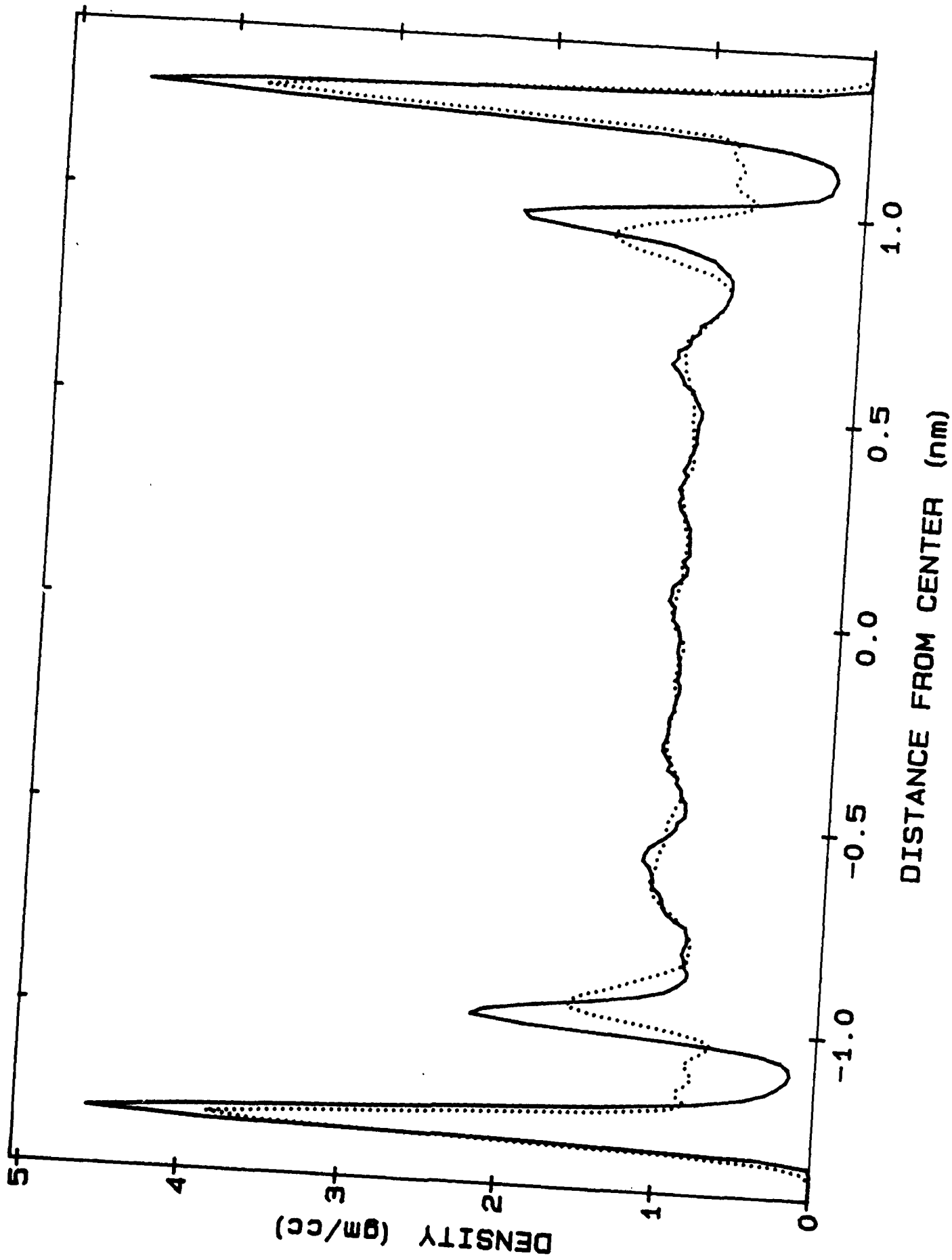
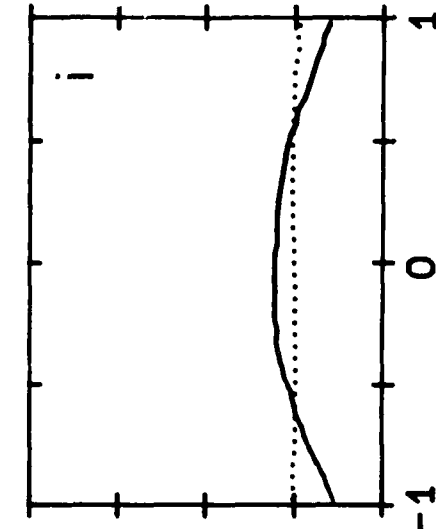
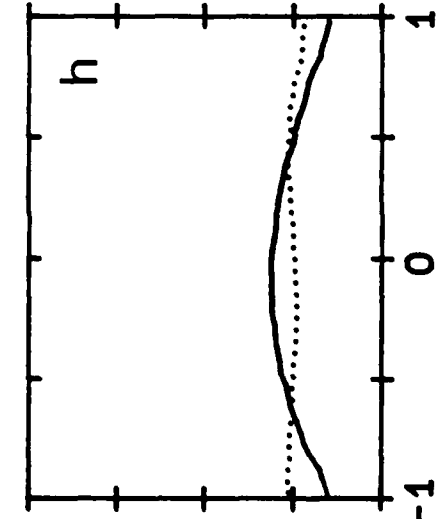
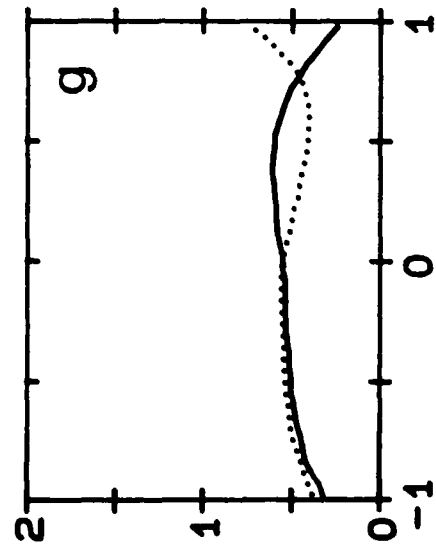
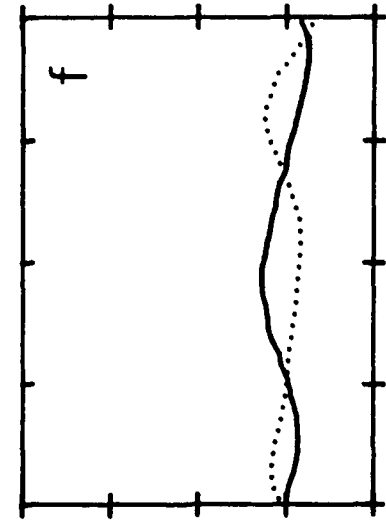
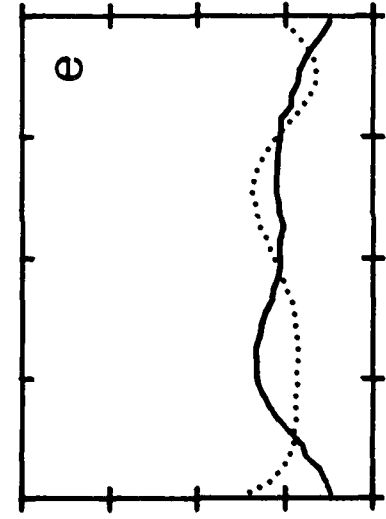
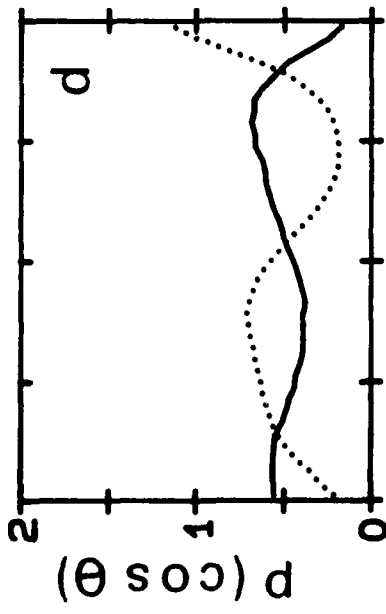
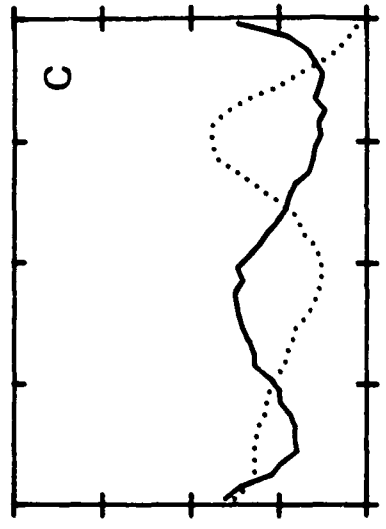
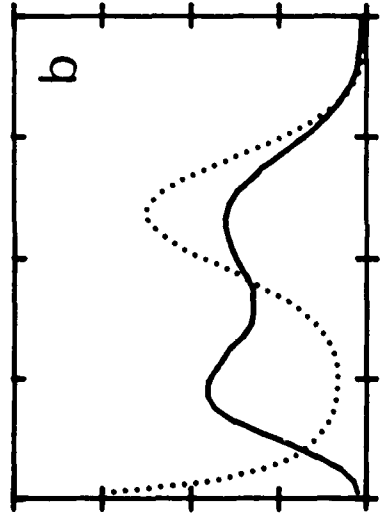
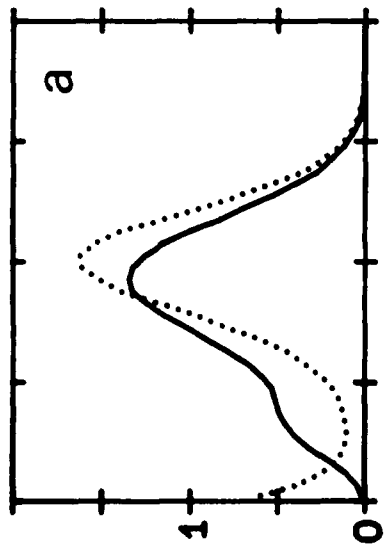


fig. 5



$\cos \theta$

fig. 6

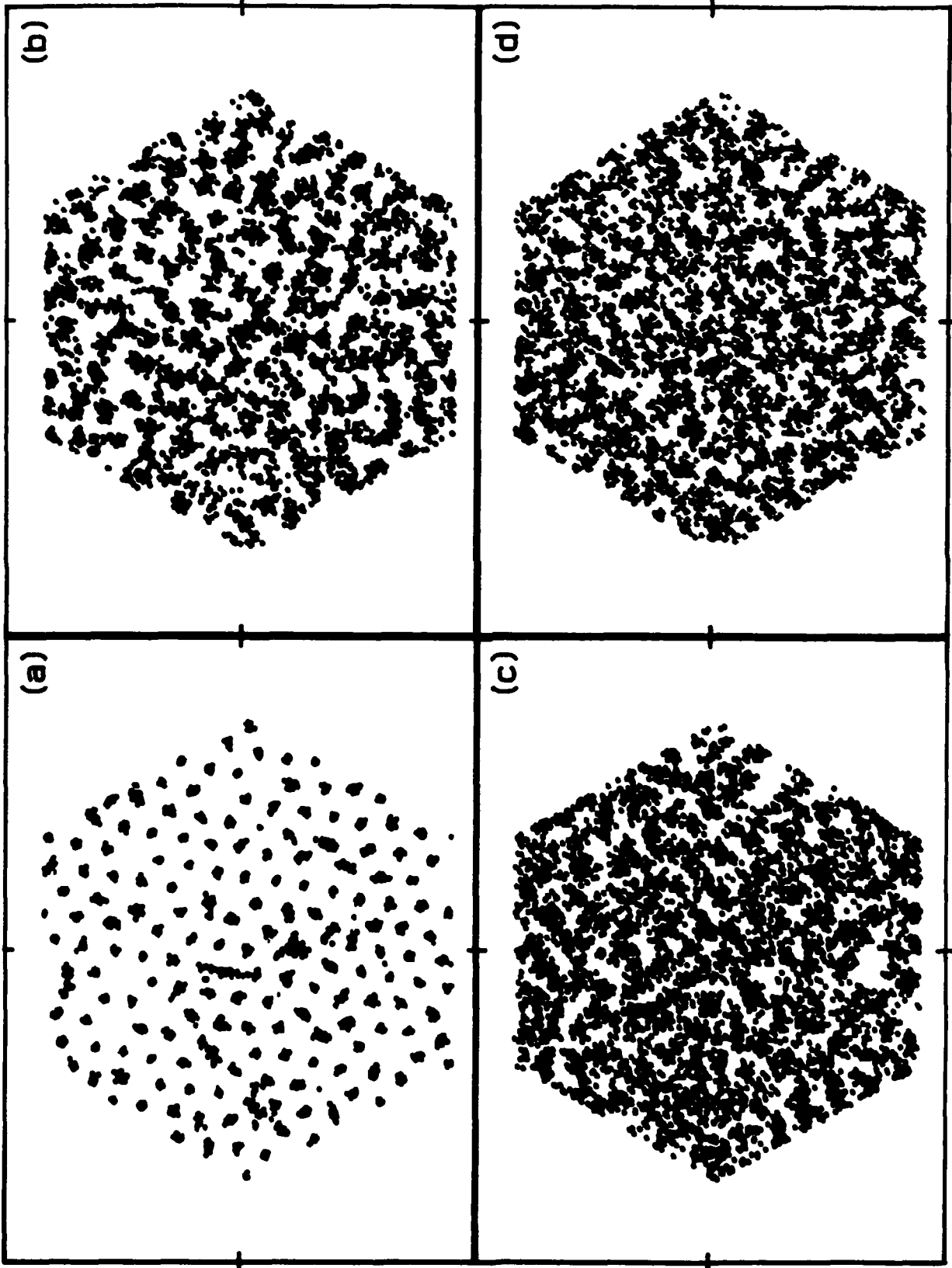


fig. 7

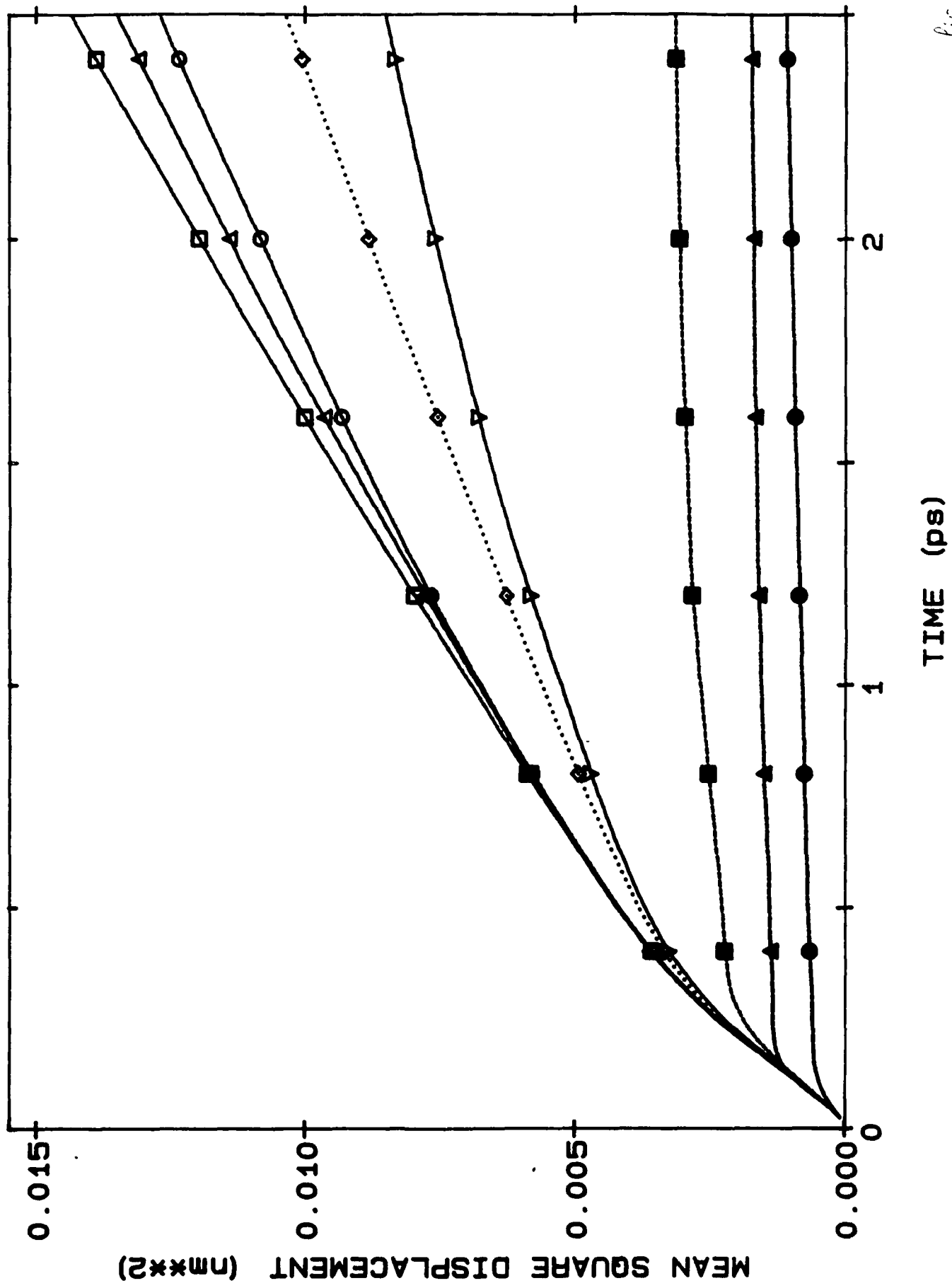
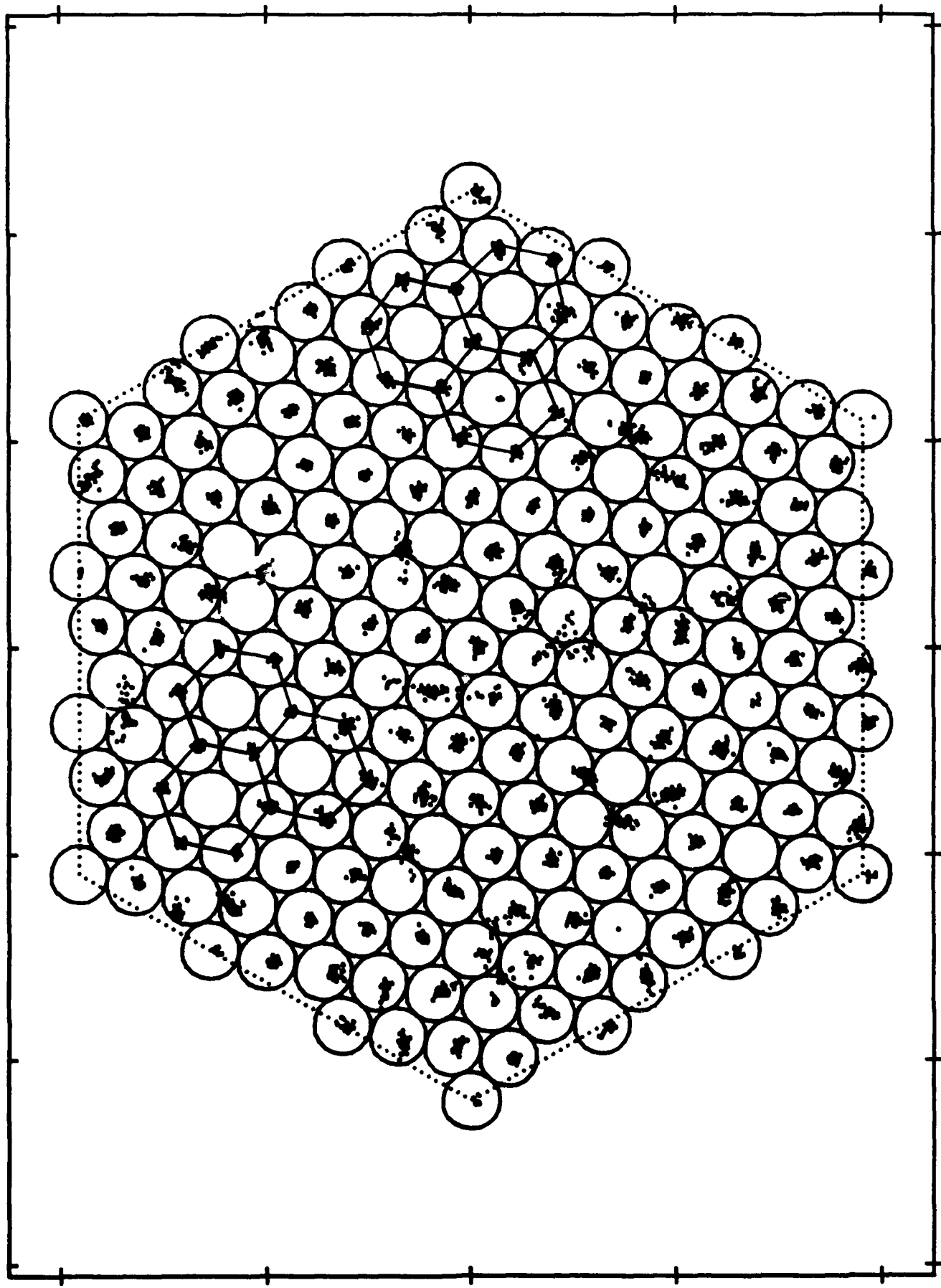
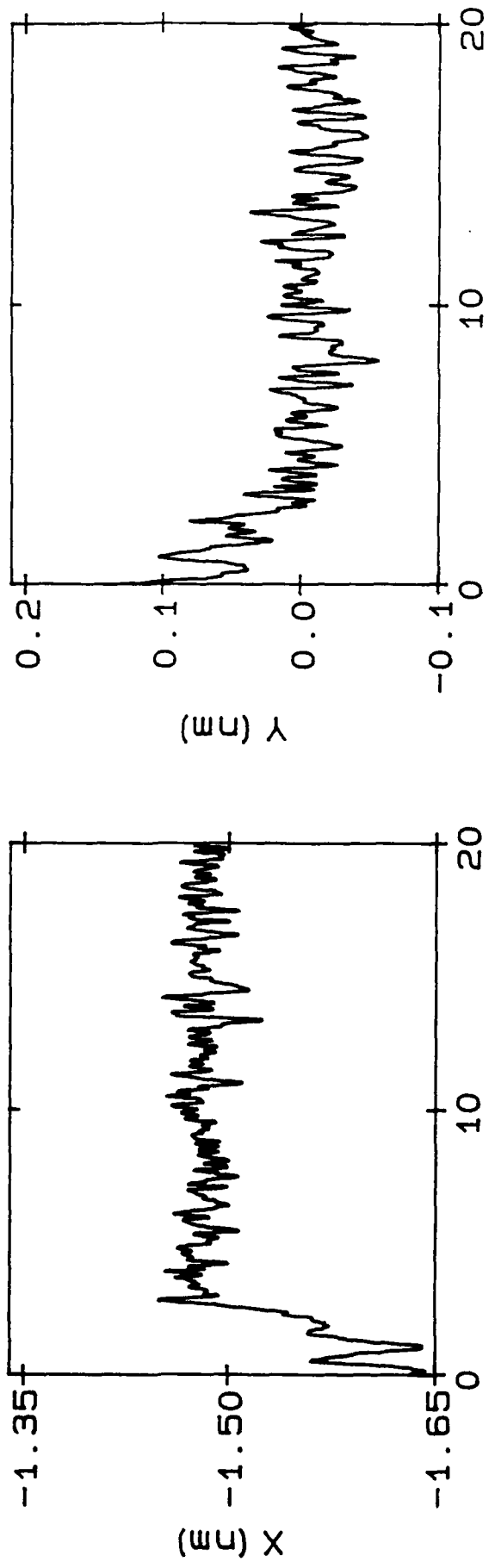


fig 8

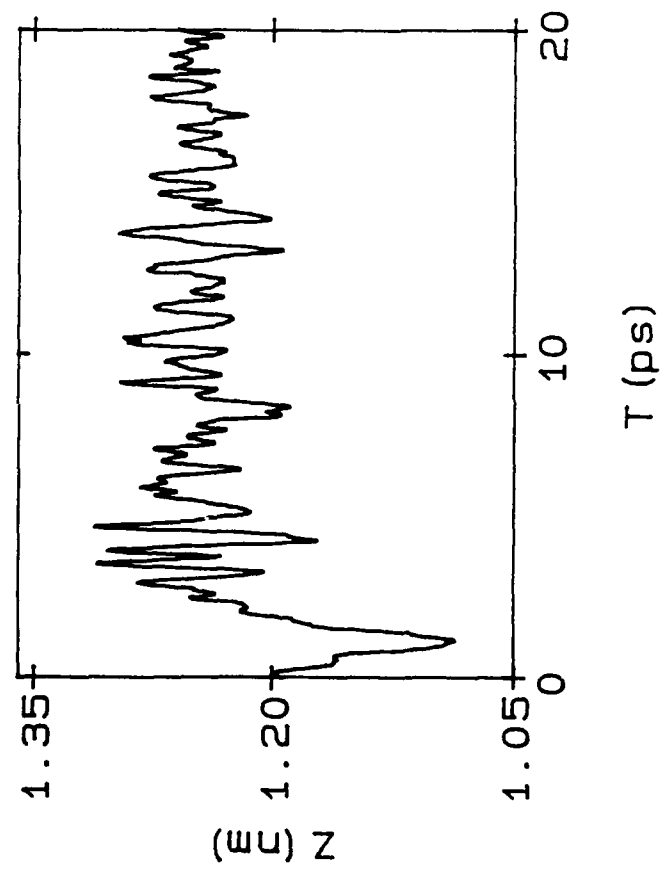
Fig. 9





$T$  (ps)

$T$  (ps)



$T$  (ps)

Fig. 10